



Breast Cancer Detection Based on Image Denoising in Multiple Modes

Zheng Yin^{1†}, Shijie Pang^{2†}, Yi Yang^{3†*}

¹ School of Computer Science, University of Nottingham, Nottingham NG7 2RD, UK

² College of Global Talents, BITZH, Beijing Institute of Technology, Zhuhai, Zhuhai, China

³ School of Informatics, University of Edinburgh, 10 Crichton Street, Edinburgh, Scotland

psxzy15@nottingham.ac.uk, stu1905305@cgt.bitzh.edu.cn, Y.Yang-174@sms.ed.ac.uk*

†These authors contributed equally.

Abstract

Breast cancer is cancer that develops from breast tissue, and it is the leading type of cancer in women. Convolutional neural network (CNN) is a very effective auxiliary method for medical image detection and classification as well as denoising, which is very important for diagnosis and analysis of medical images. In this study, DenseNet was used for breast cancer image classification and REDNet and a PRIDNet was used for image denoising. By comparing the accuracy of different input with different noise level and denoising model, this study showed that denoising can remove the redundant information of images with noise and improve the accuracy of classification and higher Peak Signal to Noise Ratio (PSNR) and Structural Similarity (SSIM) would lead to a higher classification accuracy. The model performed better on the images with similar noise to the noise of the training image.

Keywords: Image denoising, Breast cancer classification, Convolutional neural network

1 INTRODUCTION

Breast cancer is the most frequent malignant tumor in women, affecting one in every eight women around the world. However, if caught early enough, it is one of the most curable cancers. By detecting the malignant potential of breast tissue cells, the extent of tumor damage can be determined. Computer-assisted diagnosis (CAD) can increase diagnosis efficiency by assisting doctors in making accurate and timely diagnoses.

Histopathological images recorded under a microscope are processed and analyzed using various algorithms in modern medical image processing techniques. One of the approaches used to process medical images and pathology tools is machine learning algorithms. [4] [7]. Recently, computer vision technology has mainly focused on the domain related to images, such as magnetic resonance imaging (MRI), computer tomography scanning (CTs), and local pathological mapping (PM). The pathological images of mammary gland cells contain abundant phenotypic and molecular information. However, due to the diversity and complexity of pathological images, feature extraction is still difficult in feature engineering.

Therefore, it is a valuable direction that unsupervised learning can obtain features from unlabelled data, making it possible to extract organizational information automatically. The famous in the field of unsupervised learning is self-encoders. Besides, feature extraction and classification of pathological images are realized based on an unsupervised self-encoder algorithm, data generation, dimensionality reduction and visualization are completed, and the characterization ability to exist different self-encoders is sorted out [3]. Finally, the characteristics of pathological image analysis were discussed. It, therefore, makes sense to research how to reduce image noises depending on the type of medical images and the quantity of pixels.

Some deep Convolution Neural networks (CNNs) have resulted from a significant improvement in denoising [2] [5] [6] [11]. Diwakar et al. [2] concluded that the types of CT image noise include random, statistical, and electronic noise and their denoising. Nishio et al. [5] clearly introduced denoising auto-encoders (DAE) and convolutional auto-encoders (CAE). However, they did not focus on comparing the results of using different types of noise to denoise.

In this paper, the unsupervised self-encoder syndrome learning method was studied to obtain reliable breast cancer pathology syndrome under the condition of no label, thus laying a foundation for subsequent classification tasks. In the first stage, a large amount of unlabelled data is used for unsupervised learning. The quality of feature extraction of different autoencoders is compared through reconstruction and generation of autoencoders, and then the extracted features are visualised and analysed. Finally, the reliability of features is judged. In the case of pathological images, the convolution neural network is used to detect breast cancer [1]. In the last part of the paper, the experiments related to different noises were compared and concluded which is the best optimisation.

2 METHODOLOGY

2.1 Experimental Dataset

The dataset, Breast Cancer Histopathological Database (BreakHis) [8], used in this study is composed of 7, 909 images within two different classes: the benign tumour class (2, 480 images) and the malignant tumour class (5, 429 images), respectively. The benign tumour class contains four distinct histological types: adenosis (A), fibroadenoma (F), tubular adenoma (TA), and phyllodes tumour (PT); and the malignant tumour class includes four malignant tumours: ductal carcinoma (DC), lobular carcinoma (LC), mucinous carcinoma (MC), and papillary carcinoma (PC). Figure 1 shows a couple example images from this dataset.

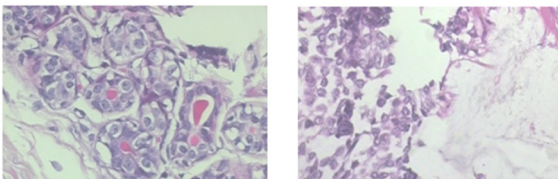


Figure 1: The example of benign tumour (left) and malignant tumour images (right).

Each image has four different magnification sizes: 40X, 100X, 200X, and 400X. This study used the 200X data to do the following classification since the 200X data gets the highest F1 score [3].

2.2 Experimental setting

In the data pre-processing step, we separately added noises to the dataset with respect to Gaussian noise and Poisson noise by using an open-source Python library, scikit-image. In the case of Gaussian noise, it is a type of statistical noise with a probability density function equal to that of a normal distribution. In the case of Poisson noise, the original value of the pixels of an image is lost.

It can be modelled by Poisson process. As a result, we got three datasets: the original dataset, Gaussian noisy and Poisson noisy datasets.

2.3 Proposed method

In order to remove the above types of noise, we used the following methods.

2.3.1 Gaussian blur

We used this filter to smooth images by convolving an image with equation (1) to reduce the noise level, and we set the standard deviation up to 1.5, and the location pair to (5, 5) in this study to limit unrelated features.

$$G = \frac{1}{2\pi\sigma^2} e^{-\frac{x^2+y^2}{2\sigma^2}} \quad (1)$$

where σ is the standard deviation of the distribution and (x, y) pair are the location indices.

2.3.2 Box linear filter

Box blur with the five by five (5×5) convolutional kernel was used that the value of each pixel in the resulting image is equal to the average value of its neighbouring pixels in the input image.

2.3.3 Residual Encoder-Decoder Network

Residual Encoder-Decoder Networks (RED-Net) is generally used to stimulate the original image of a corrupted image. Typically, the relation between the authentic and corrupted images can be shown as $Y=D+N$, where Y is pixel sets of corrupted images, D is the degradation of the set of the stimulated original image, and N is the additive noise. Based on that relation, RED-Net is defined as a particular deep neural network that contains symmetric encoder and decoder layers. The encoder eliminates noises after capturing the abstraction of the image. The decoder works like a feature extractor. Because of this coarse-to-fine structure, we could concrete the input features five times and then restore the lost information gradually by handling five encoder layers and five decoder layers overall.

2.3.4 Pyramid Real Image Denoising Network

PRIDNet is an advanced deep learning architecture for blind noise reduction [10] shown in Figure 2. It is divided into three main parts, such as, Channel attention module architecture, multi-scale feature extraction and Kernel selecting module architecture.

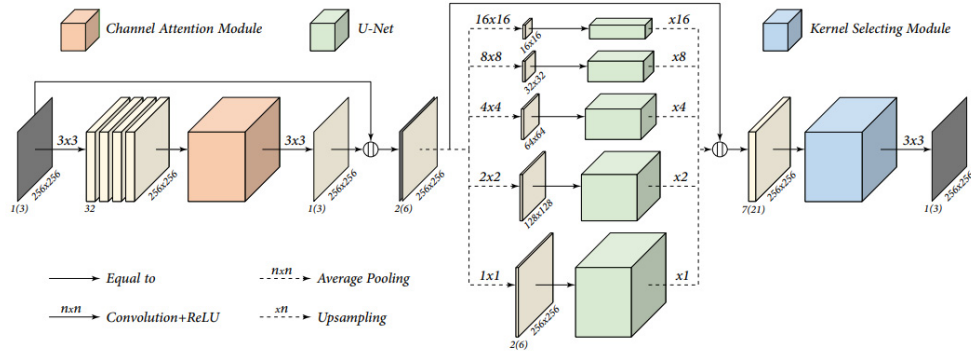


Figure 2: The architecture of PRIDNet [10].

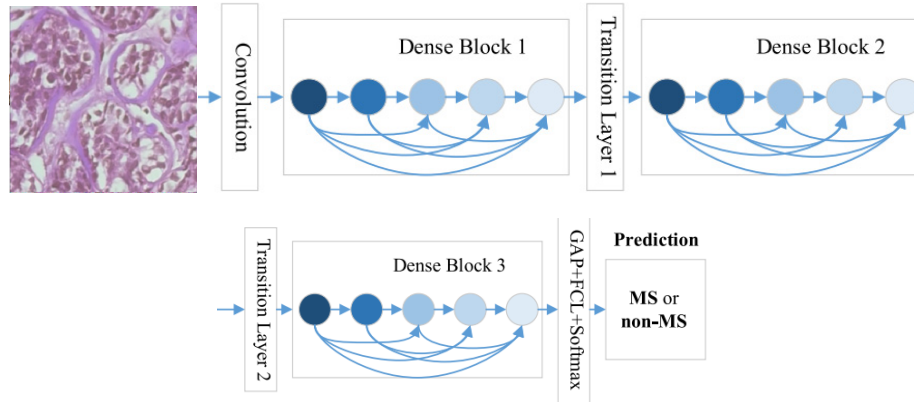


Figure 3: Relation of Dense Blocks and Transition Layers (GAP = global average pooling; FCL = fully connected layer; MS = multiple sclerosis).

Two fully connected layers (FC) transmit the input U using global average pooling (GAP), which results in the output as shown in (2)

$$\mu = \text{Sigmoid}(\text{FC2}(\text{ReLU}(\text{FC1}(\text{GAP}(U)))) \tag{2}$$

Then, using U-Net architecture in each pooled feature, is in favour of up sampling with same size kernel in the average pooling, and then it can recover the size of the output image to the initial image. The last part, in order to choose different size on kernel, involves kernel selecting module. Creating different branches, this means that different attention to these branches results in different sizes of effective receptive fields of neurons in the fusion layer. As indicated in equation, the final output feature graph V is calculated by merging each kernel and its attention weights (3).

$$V_c = \alpha_c \cdot U' + \beta_c \cdot U'' + \gamma_c \cdot U''' \tag{3}$$

2.4 Convolutional Neural Networks

A convolutional neural network (CNN) is a class of Artificial Neural networks (ANN), most applied to analyse visual imagery. The Convolution neural network is mainly composed of the input layer, convolution layer,

activation function (i.e. ReLu), pooling layer, full connection layer, and loss function. Skip connections, or shortcuts, are used by a residual neural network (i.e. ResNet) to jump over some layers. ResNet models are commonly constructed with batch normalization and double- or triple-layer skips incorporating nonlinearities (ReLU) (Figure 4). There are two main reasons to add skip connections: to avoid vanishing gradients or to ameliorate the Degradation (accuracy saturation) problem, which occurs when adding more layers to a sufficiently deep model results in increased training error.

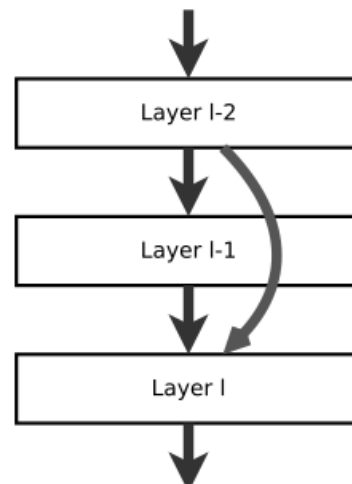


Figure 4: ResNet layer mechanism.

2.5 Densely Connected Convolutional Networks

The DenseNet model builds a dense connection between all previous layers and subsequent layers. Feature reuse is characterized by the linking of features on channels. As a result, DenseNet can outperform ResNet with fewer parameters and lower computing costs. [9].

DenseNet will connect all the previous layers as input as shown in formula (4),

$$x_l = H_l([x_0, x_1, \dots, x_{l-1}]) \quad (4)$$

and then each input is connected in the channel dimension.

In order to ensure the feature graph size of DenseNet can be kept consistent. The structure of DenseBlock and Transition is used in the DenseNet network, and each DenseBlock is connected through Transition, so that, Figure 3, shows how to conduct batch normalization, convolution, and pooling procedures.

3 EXPERIMENT AND RESULTS

In the study, the original size of the picture is 700×460 pixels. The Densely Connected Convolutional Networks (DenseNet) was trained for classification in the first stage. When loading the cancer images, we resized the image to 389×256 . The input size of the DenseNet was 224×224 , so we captured the upper left 224×224 corner of the images as the input, trained the model and got the accuracy. And then, we added Gaussian noise in the images with the noise level (var: Variance of random distribution) $\text{var}=0.01$, $\text{var}=0.05$, $\text{var}=0.1$, $\text{var}=0.2$, trained the model independently and got the accuracy.

In the next part, the RED-Net was trained for denoising; the input size of the model is 256×256 . Normal images and images with noise were sent to the model as input. Gaussian noise with the noise level ($\text{var}=0.01$, $\text{var}=0.05$, $\text{var}=0.1$, $\text{var}=0.2$) and Poisson noise was added to the images, and images with different noise were trained in the model independently. After training the model, the dataset with noise was sent to the model as the input, and the denoised images were obtained. The peak signal to noise ratio (PSNR) and structural index similarity (SSIM) were calculated, and the denoised images were sent to the CNN classifier to compare the classification accuracy.

The PRIDNet was trained like REDNet. The difference is that the input size of PRIDNet is 40×40 . The model was trained, and images were sliced into 40×40 squares during denoising and recombined after denoising.

Table 1: Accuracy of five noise levels on noised, RED, PRID models

Noise level	0	0.01	0.05	0.1	0.2
noised	88.1%	84.2%	83.5%	82.3%	81.5%
RED	-	87.5%	86.9%	85.6%	83.9%
PRID	-	87.9%	85.7%	84.5%	82.6%

Table 2: PSNR of four noise levels on noised, RED, PRID models

Noise level	0.01	0.05	0.1	0.2
noised	20.11	13.83	11.49	9.59
RED	26.53	26.44	24.96	23.36
PRID	29.48	23.74	22.09	21.10

Table 3: SSIM of four noise levels on noised, RED, PRID models

Noise level	0.01	0.05	0.1	0.2
noised	0.4393	0.1705	0.1030	0.0623
RED	0.7663	0.7640	0.6939	0.5993
PRID	0.867	0.6454	0.5499	0.4755

At last, we got the classification accuracy, PSNR, and SSIM. The image in the first row of Figure 3 is the original image. The images shown in the second row of Figure 5, were added 0.01, 0.05, 0.1 and 0.2 Gaussian noise in the 1st, 2nd, 3rd and 4th columns respectively. The result images after RED-Net and PRIDNet denoising are also shown in the third and fourth row respectively. The accuracy result of the CNN classification network did not converge to the same value every time as shown in Table 1. We, therefore, trained the model with each data with a different noise level and denoising method several times and calculated the average accuracy, after which the PSNR and SSIM value was the value of one image. The results show that the pre-processing denoising can remove the redundant information of images and improve the accuracy of classification. Table 2 and Table 3 show that the images having higher PSNR and SSIM tend to have a higher classification accuracy.

Table 4: PSNR and SSIM values on models with 4 levels of Gaussian noise and Poisson noise.

Model	PSNR	SSIM
Noise	9.599	0.0611
0.2 Gaussian	23.122	0.5927
0.1 Gaussian	22.097	0.5889

0.05 Gaussian	21.100	0.5620
0.01 Gaussian	19.106	0.4375
Poisson	18.008	0.3508
Gaussian blur	19.308	0.4356
Box blur	19.463	0.4202

Then we choose the image with Gaussian noise level $\text{var} = 0.2$ and use pre-trained images to denoise the image. We also used traditional Gaussian blur and Box blur to denoise the image. The denoised image can be found in Figure 6. The model trained with the same noise level performed the best, and the closer the noise level of the model was, the better the model performed. And the model trained with Gaussian noise performed better than the model trained with Poisson noise. If the training noise differs a lot from the target noise, the model could perform worse than traditional filters. It shows that the denoising device has a strong denoising ability to the same noise as the training set noise.



Figure 5: Examples of Denoised images.

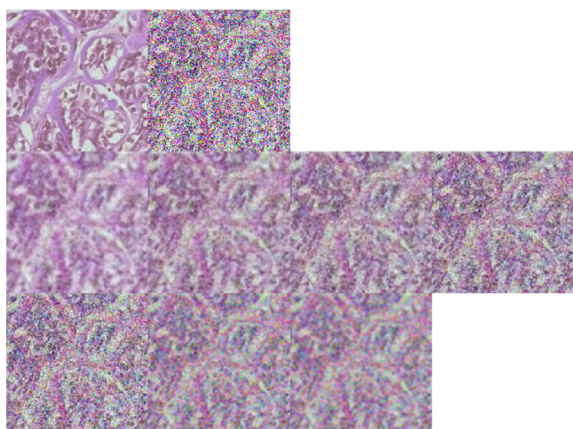


Figure 6: Examples of Denoised images.

The images in 1st row: the left one is the original image and the right one is the image with 0.2 Gaussian

noise. The second row are the result of denoising on models which were trained with 0.2, 0.1, 0.05, 0.01 Gaussian noise respectively. The third row is the result of denoising on model which was trained with Poisson noise and the denoising result of Gaussian blur and Box blur.

4 CONCLUSIONS

This study used a DenseNet for breast cancer image classification and used a REDNet and a PRIDNet for image denoising. The results have shown that denoising can remove the redundant information of images with noise and improve the accuracy of classification. The images having higher PSNR and SSIM tend to have a higher classification accuracy. Our future work would focus on how to improve the denoising performance, and whether a model which can get a good performance on an image set with different kinds of noise can be implemented.

REFERENCES

- [1] Albawi, S., Mohammed, T. A., & Al-Zawi, S. (2017, August). Understanding of a convolutional neural network. In 2017 international conference on engineering and technology (ICET) (pp. 1-6). Ieee.
- [2] Diwakar, M., & Kumar, M. (2018). A review on CT image noise and its denoising. *Biomedical Signal Processing and Control*, 42, 73-88.
- [3] Gour, M., Jain, S., & Sunil Kumar, T. (2020). Residual learning based CNN for breast cancer histopathological image classification. *International Journal of Imaging Systems and Technology*, 30(3), 621-635.
- [4] Kisilev, P., Sason, E., Barkan, E., & Hashoul, S. (2016). Medical image description using multi-task-loss CNN. In *Deep learning and data labeling for medical applications* (pp. 121-129). Springer, Cham.
- [5] Nishio, M., Nagashima, C., Hirabayashi, S., Ohnishi, A., Sasaki, K., Sagawa, T., ... & Yamashita, T. (2017). Convolutional auto-encoder for image denoising of ultra-low-dose CT. *Heliyon*, 3(8), e00393.
- [6] Qiu, Y., Yang, Y., Lin, Z., Chen, P., Luo, Y., & Huang, W. (2020). Improved denoising autoencoder for maritime image denoising and semantic segmentation of USV. *China Communications*, 17(3), 46-57.
- [7] Sarvamangala, D. R., & Kulkarni, R. V. (2021). Convolutional neural networks in medical image understanding: a survey. *Evolutionary intelligence*, 1-22.

- [8] UFPR (2017). Breast Cancer Histopathological Database (BreakHis), <https://web.inf.ufpr.br/vri/databases/breast-cancer-histopathological-database-breakhis/>
- [9] Wang, S. H., & Zhang, Y. D. (2020). DenseNet-201-based deep neural network with composite learning factor and precomputation for multiple sclerosis classification. *ACM Transactions on Multimedia Computing, Communications, and Applications (TOMM)*, 16(2s), 1-19.
- [10] Zhao, Y., Jiang, Z., Men, A., & Ju, G. (2019, December). Pyramid real image denoising network. In *2019 IEEE Visual Communications and Image Processing (VCIP)* (pp. 1-4). IEEE.
- [11] Zhang, K., Zuo, W., & Zhang, L. (2018). FFDNet: Toward a fast and flexible solution for CNN-based image denoising. *IEEE Transactions on Image Processing*, 27(9), 4608-4622.

Open Access This chapter is licensed under the terms of the Creative Commons Attribution-NonCommercial 4.0 International License (<http://creativecommons.org/licenses/by-nc/4.0/>), which permits any noncommercial use, sharing, adaptation, distribution and reproduction in any medium or format, as long as you give appropriate credit to the original author(s) and the source, provide a link to the Creative Commons license and indicate if changes were made.

The images or other third party material in this chapter are included in the chapter's Creative Commons license, unless indicated otherwise in a credit line to the material. If material is not included in the chapter's Creative Commons license and your intended use is not permitted by statutory regulation or exceeds the permitted use, you will need to obtain permission directly from the copyright holder.

